

Supplementary Information

Cobalt-doped porphyrin-based porous organic polymer-modified separator for high-performance lithium–sulfur batteries

Shunyou Hu^a, Mingjie Yi^a, Xiyan Huang^a, Dong Wu^a, Beibei Lu^a, Tiansheng Wang^a, Na Li^a, Zhenye Zhu^a,
Xiangli Liu^{c*}, Jiaheng Zhang^{a,b *}

^a*Research Centre of Printed Flexible Electronics, School of Materials Science and
Engineering, Harbin Institute of Technology,
Shenzhen 518055, China*

^b*State Key Laboratory of Advanced Welding and Joining, Harbin Institute of
Technology, Shenzhen 518055, China.*

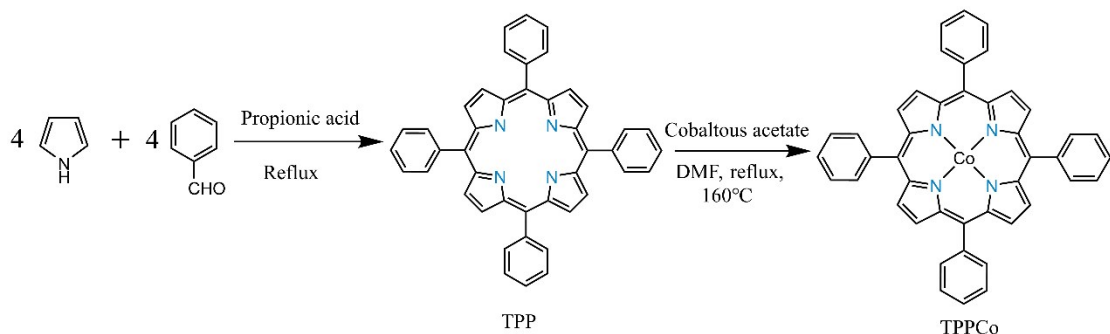
^c*Shenzhen Engineering Laboratory of Aerospace Detection and Imaging, Department
of Materials Science and Engineering, Harbin Institute of Technology (Shenzhen),
Shenzhen 518055, China*

Corresponding author:

Jiaheng Zhang, Email: zhangjiaheng@hit.edu.cn

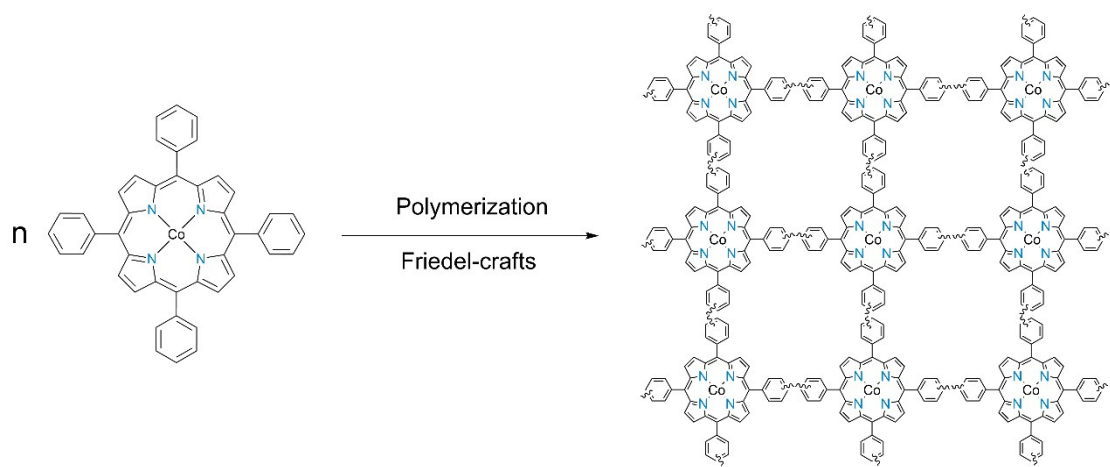
Xiangli Liu, Email: xiangliliu@hit.edu.cn

1. Synthesis of TPP



Scheme 1. The synthesis process of TPP and TPPCo.

TPP: In a typical way, benzaldehyde (50 mmol) was added to a two-necked round-bottomed flask (250 mL) containing 120 mL of propionic acid, and heated to 140°C, followed by addition of freshly distilled pyrrole (50 mmol). After refluxing for 2 h, the solution was cooled to room temperature naturally and added 120 mL of absolute ethanol. Subsequently, the as-obtained precipitate was filtered, washed with methanol and dried in the room temperature. The precipitate was further purified with silica gel column chromatography using CH₂Cl₂ as eluent. After removal of eluent by rotary evaporation, the product was dried at 80 °C in vacuum for 24 h and gave the purple powder (TPP).



Scheme 2. The synthesis of PTPPCo using procedures from He and co-workers.¹

2. Shuttle current test

For the shuttle current test, LiNO₃-free electrolyte was employed to prevent the passivation of Li anode. First, batteries were galvanostatic charge to 2.8 V at 0.2 C current density. Then, the batteries were galvanostatic discharge to 2.38 V to monitor the current changes. After about 25000 s, the current was stable within a fixed range which is regarded as shuttle current².

3. Calculations of specific energy density

The gravimetric energy density was calculated from the following formula.^{3,4}

$$W_{cell} = \frac{E_{cell} \times Q \times m_s}{(m_{Li})_{anode} + (m_s)_{cathode}} \quad (\text{Equation 1})$$

$$P_{cell} = W_{cell} \times C \text{ rate } (h^{-1}) \quad (\text{Equation 2})$$

Where W_{cell} is the energy density (Wh kg⁻¹), E_{cell} is the average reversible potential (vs. Li/Li⁺), Q is the specific capacity of sulfur (mAh g⁻¹), m_s is the mass of sulfur in the cathode, m_{Li} is the mass of Li electrode (100% excess), P_{cell} is the power density (W kg⁻¹).

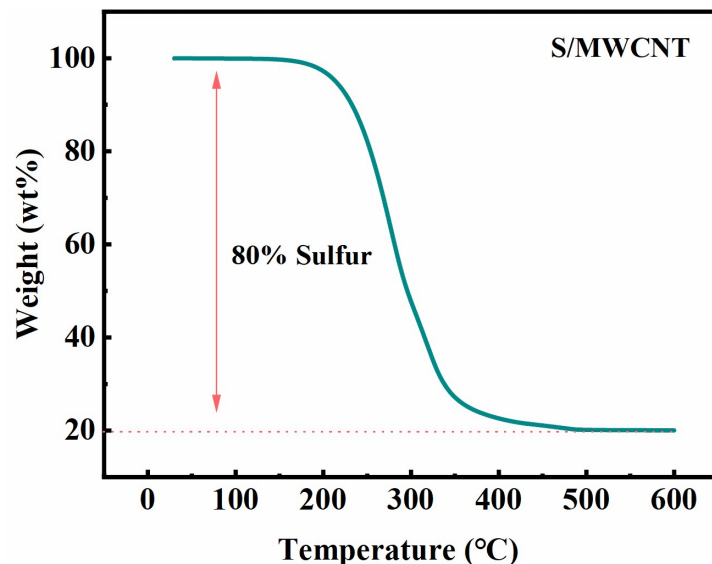


Fig. S1. TG curve of S/MWCNT composite.

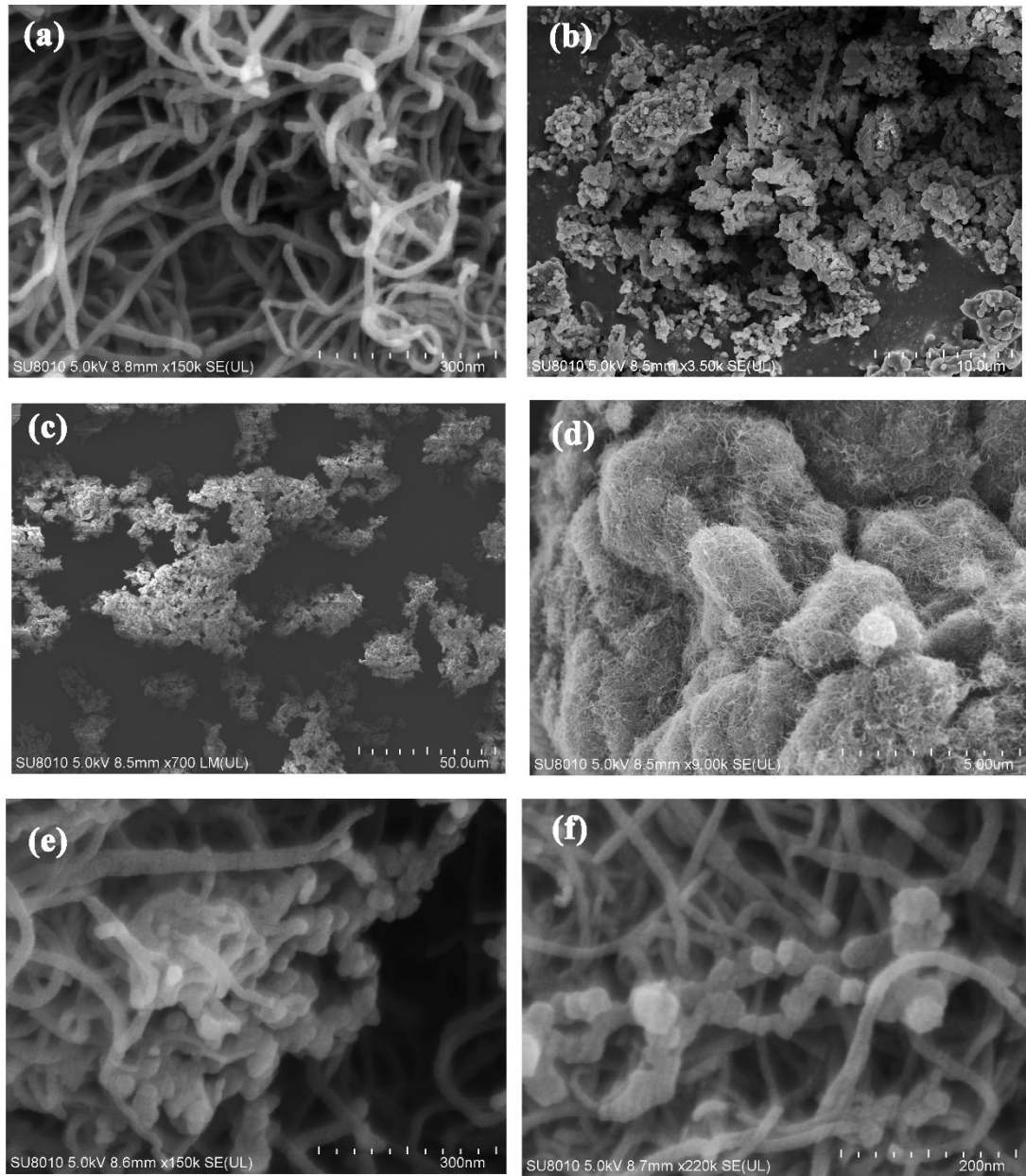


Fig. S2. SEM images of MWCNT (a), PTPPCo (b, c), PTPPCo/MWCNT(d-f).

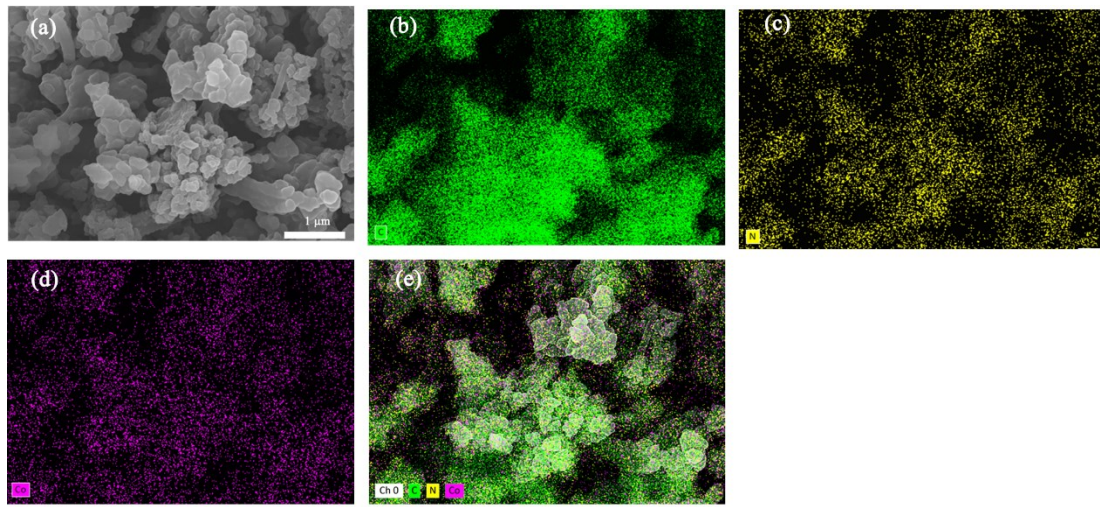


Fig. S3. Elemental mapping images of the PTPPCo.

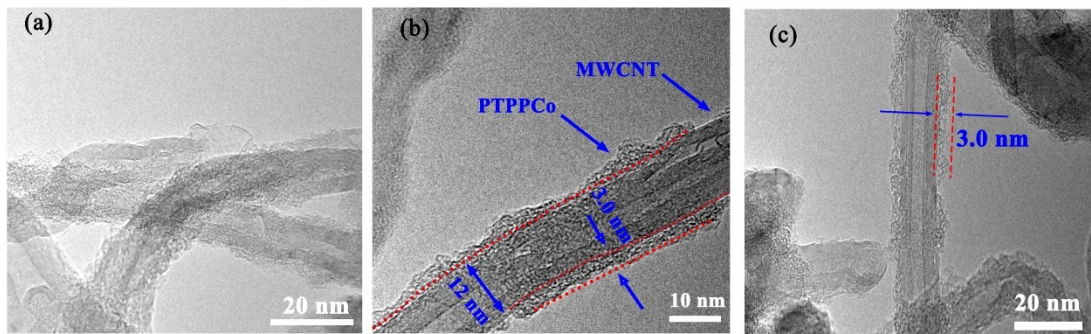


Fig. S4. The TEM images of PTPPCo/MWCNT.

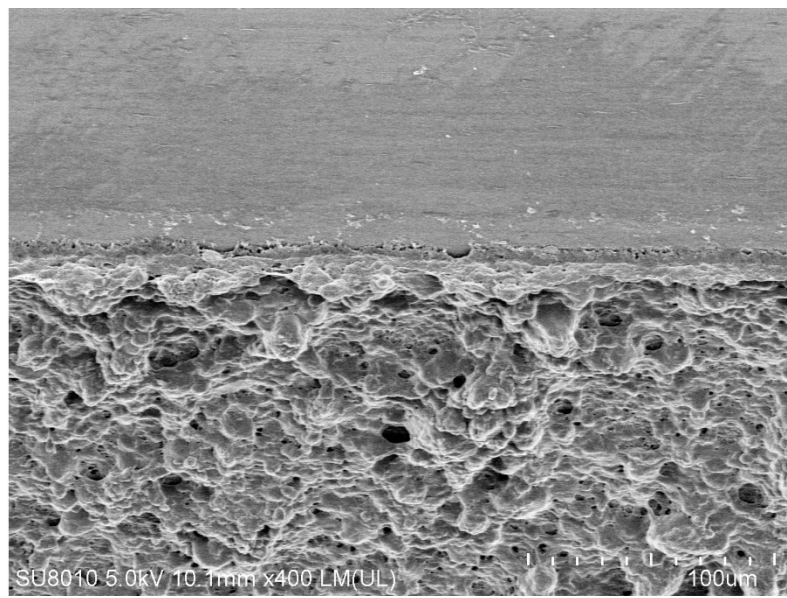


Fig. S5. SEM images of PTPPCo/MWCNT separators.

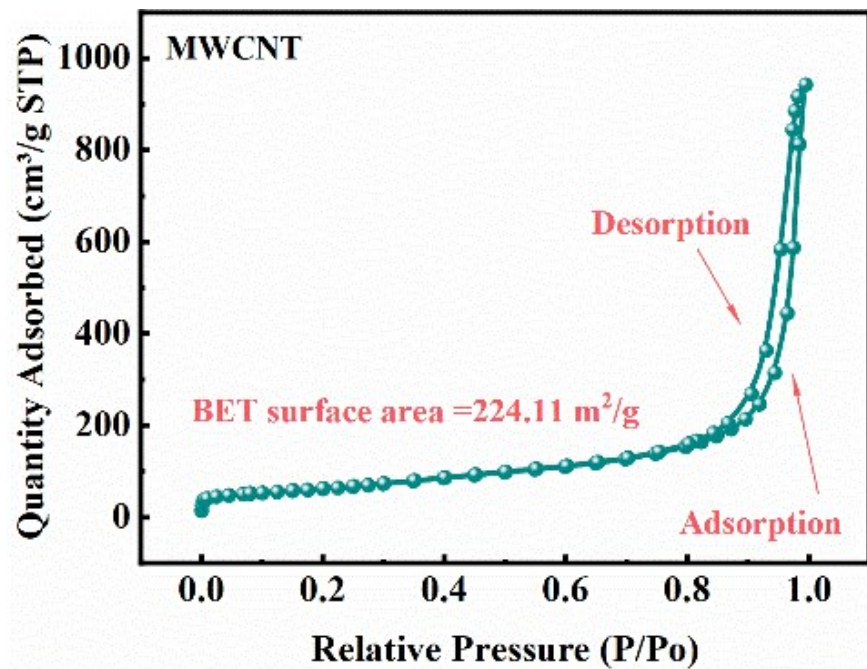


Fig. S6. Adsorption-desorption isotherms of MWCNT.

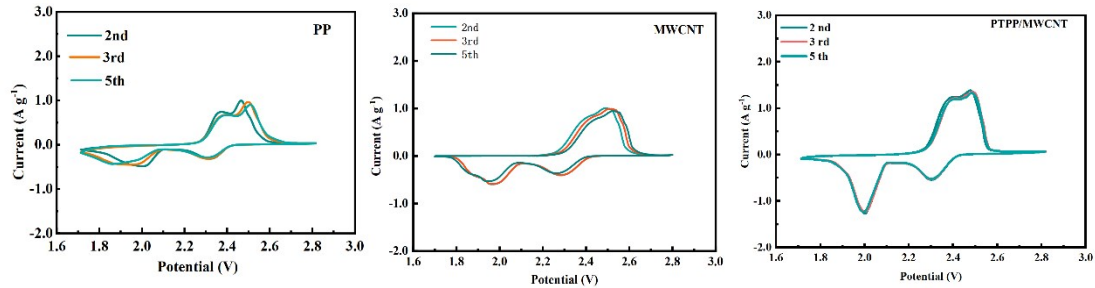


Fig. S7. CV curves of Li-S cells at 0.1 mV/s .

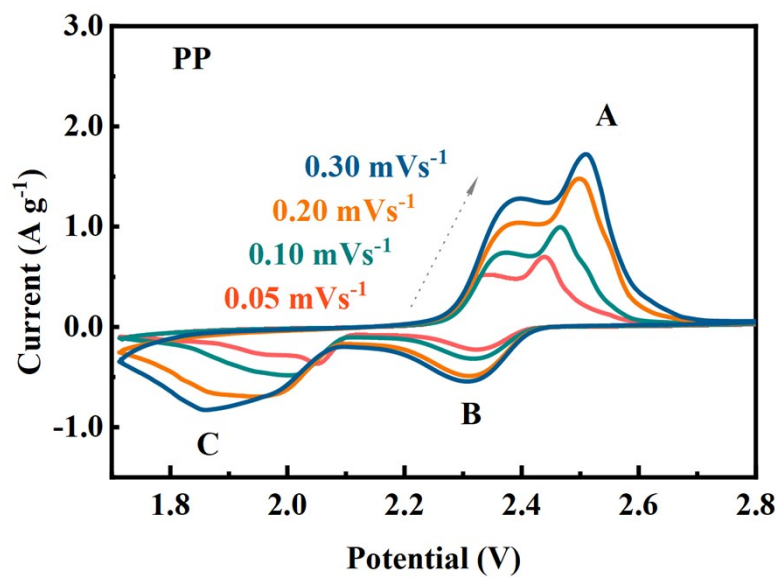


Fig. S8. CV curves of PP at various scan rate.

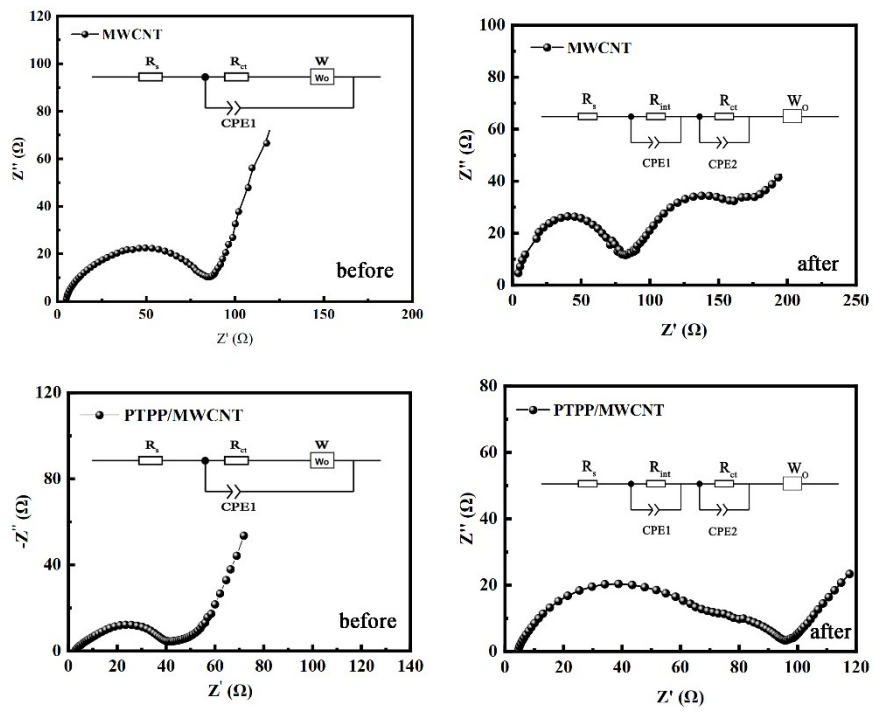


Fig. S9. The EIS of the cells with MWCNT and PTPP/MWCNT before and after cycling.

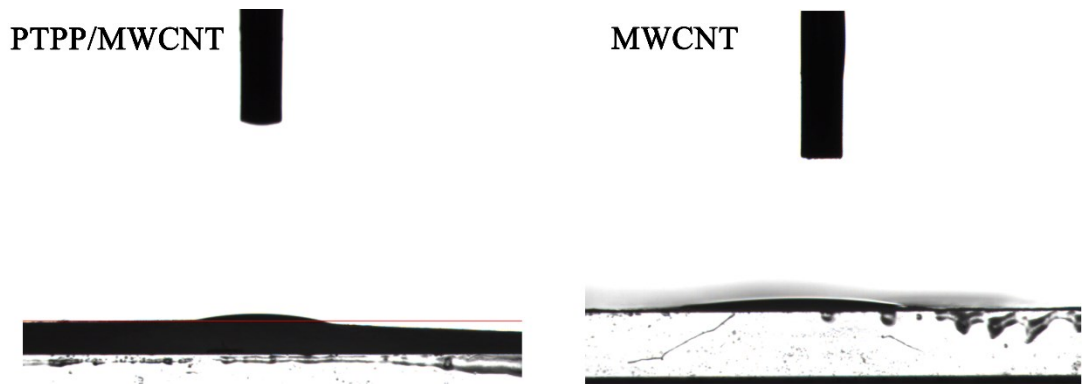


Fig. S10. The contact angle of PTPP/MWCNT and MWCNT.

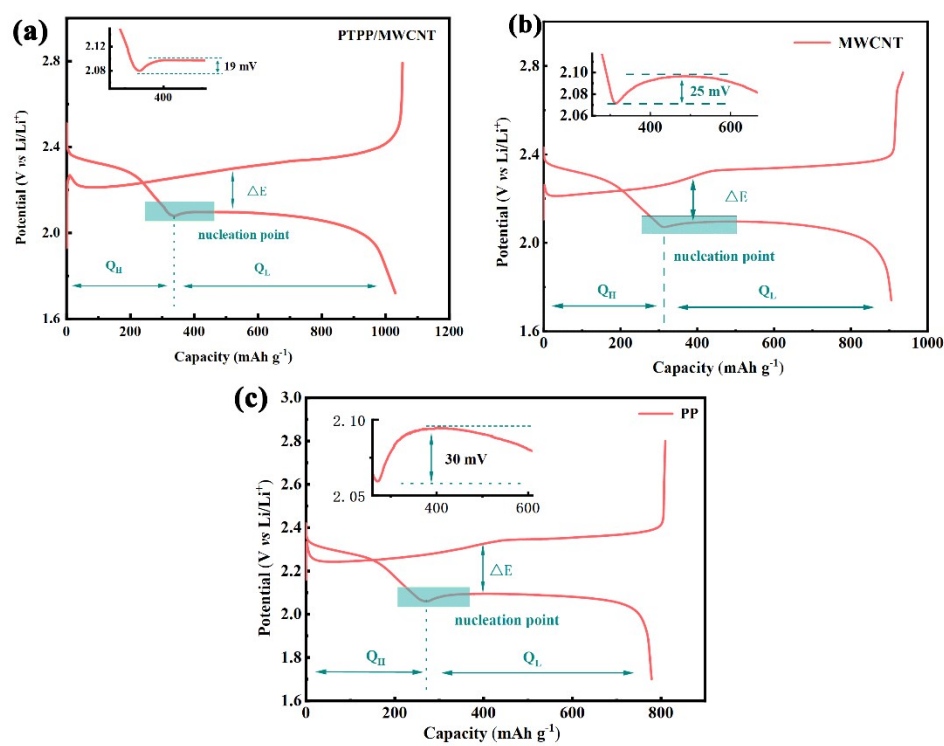


Fig. S11. Galvanostatic discharge-charge profiles of PTPP/MWCNT (a), MWCNT (b) and PP (c) separators.

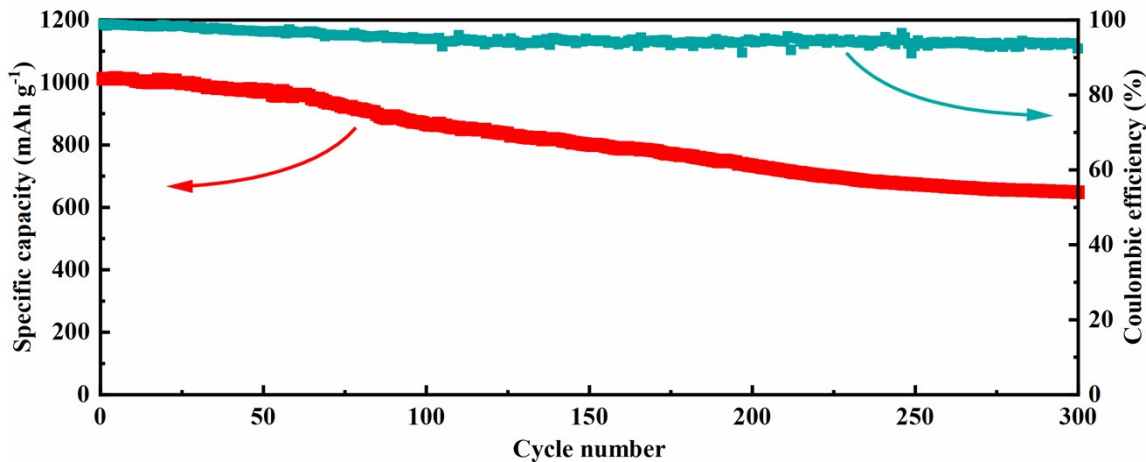


Fig. S12. Cycle stability and Coulombic efficiency at 0.5 C rate for 300 cycles using the cathode with 3 mg cm^{-2} sulfur loading.

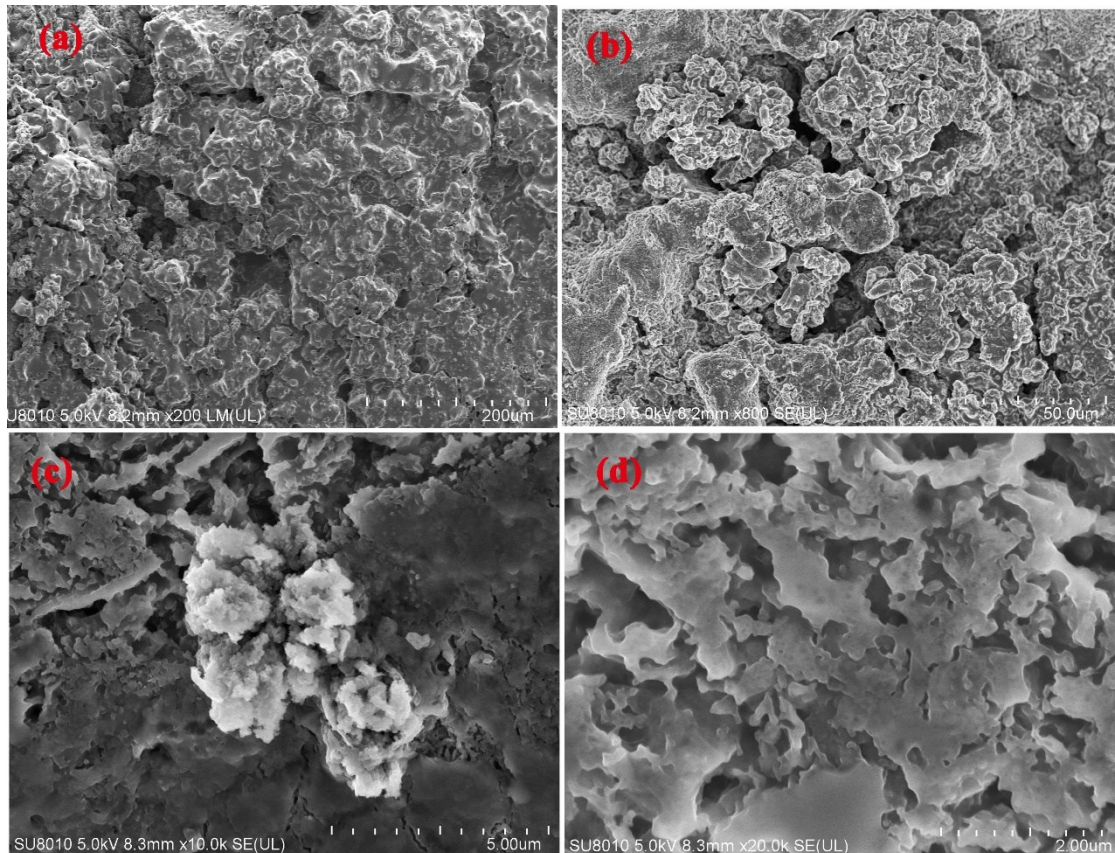


Fig. S13. SEM images of Li anodes from the cells with MWCNT (a, b) and PP (c, d) separators after cycles.

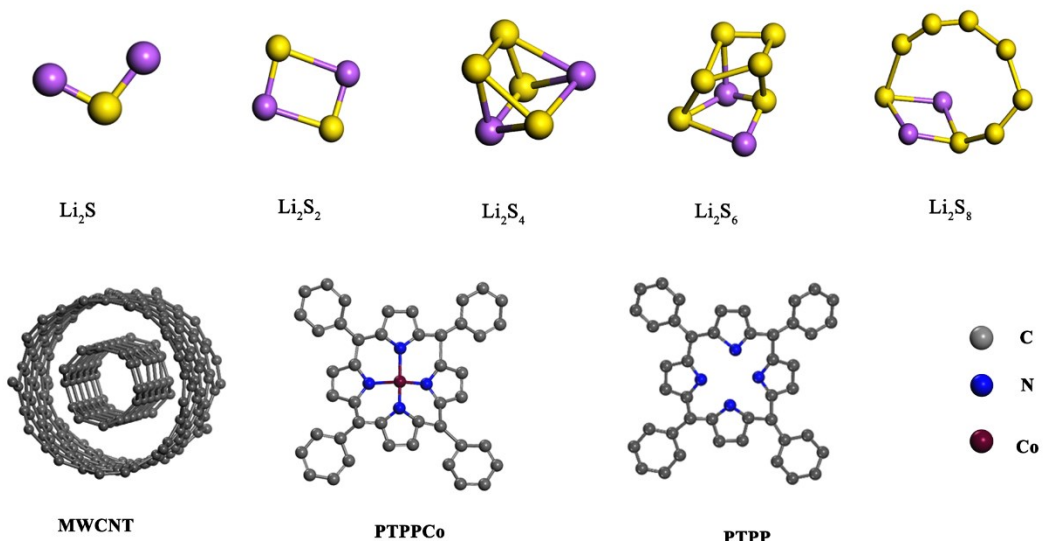


Fig. S14. Optimized constructions of polysulfides, MWCNT, TPP and TPPCo (the unit of the TPPCo).

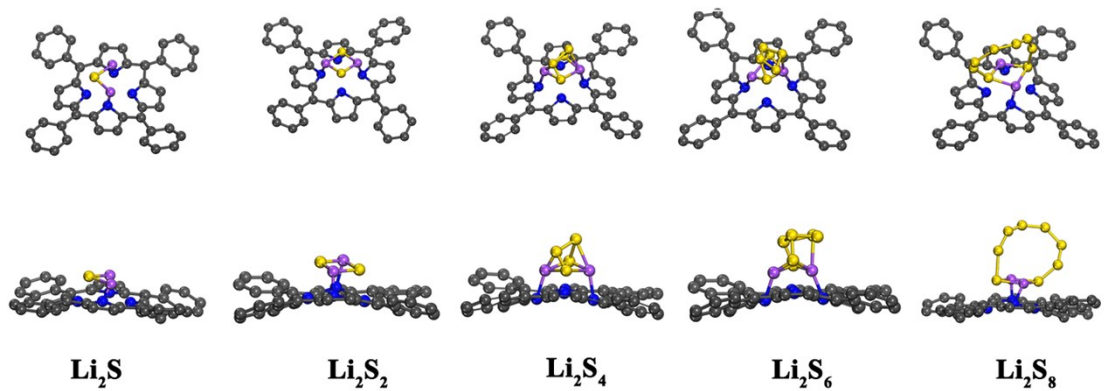


Fig. S15. Optimized chemisorption structures of TPP with polysulfides.

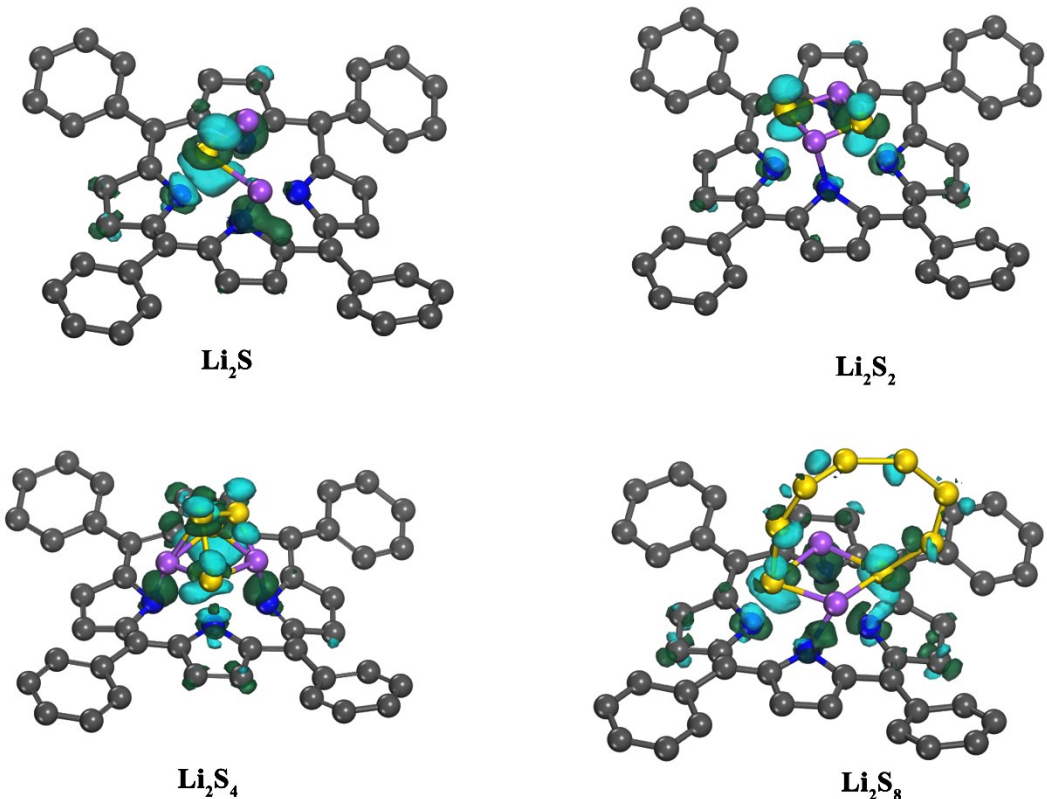


Fig. S16. Map of charge density difference of polysulfides adsorbed on PTPP. Light green denoted the decrease of electronic and dark green denoted electronic accumulation.

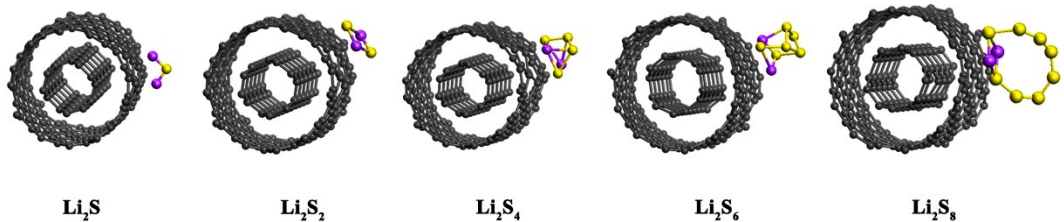


Fig. S17. Optimized chemisorption structures of MWCNT with polysulfides.

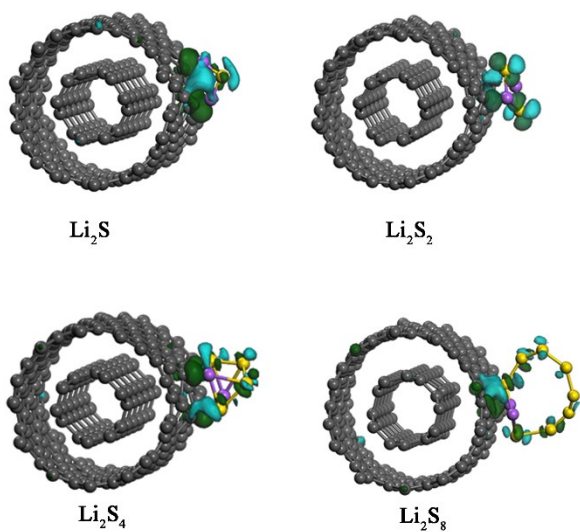


Fig. S18. Map of charge density difference of polysulfides adsorbed on MWCNT. Light green denoted the decrease of electronic and dark green denoted electronic accumulation.

Table S1. Battery performance comparison of different coating modified separator in Li-S battery.

Coating Materials	Thickness (μm)	S loading (mg cm^{-2})	Rate	Capacity (mAh g^{-1})	Operation voltage window (V)	Ref.
FHCS/PP	25	1.2	0.2	1427	1.7–2.8	5
Carbon aerogel/PP	13	0.4	0.1	1216	1.7–2.8	6
AB-CoS ₂ /PP	12	1.5	0.2	1108	1.6–2.8	7
CNTOH/PE	8.4	3	0.5	1056	1.7–2.8	8
CNF/CoS/KB/PP	10	1.8	0.1	1230	1.5–3.0	9
CNTs/MXene/PP	2.7	0.7	0.1	1415	1.7–2.8	10

HCNF/MnO ₂ /PP	2	2.0	0.2	1156	1.7–2.8	¹¹
Fe ₃ O ₄ /RGO/PP	26	0.6	0.3	850	1.7–2.8	¹²
MnO ₂ /CNT/PP	10	0.8	0.5	878.5	1.7–2.8	¹³
MOF(Ni ₃ (HITP) ₂ /PP	0.34	3.5	0.2	1186	1.7–2.8	¹⁴
MOF(UiO-66)/PP	20	1.5	0.5	1032	1.7–2.8	¹⁵
VN/PP	25	1.4-1.6	0.2	1280	1.7–2.8	¹⁶
Mxene@Nafion/PP	1	2.0	0.2	1234	1.7–2.8	¹⁷
CoN _x @NPC/G/PP	25	90 wt%	0.2	1103	1.7–2.8	⁵
Ce-MOF/CNT/PP	8	2.5	0.4	1021.8	1.7–2.8	¹⁸
2D MoS ₂ /PP	0.35		0.5	808	1.7-2.8	¹⁹
Co ₉ S ₈ /PP			1	986	1.7-2.8	²⁰
Co-N-C/rGO/PP			0.5	865	1.7-2.8	²¹
PVDF/PSSLi			0.5	955	1.7-2.8	²²
GPE/PVDF-HFP			0.1	895	1.7-2.8	²³
PAN@APP			1	790	1.7-2.8	²⁴
PAN/GO			0.2	987	1.7-2.8	²⁵
GPE/PMMA			0.3	986	1.7-2.8	²⁶
OV _S -TiO ₂	0.5	66.7 wt%	2.0	631	1.7-2.8	²⁷
F-dopped PMIA		80 wt%	2.0	750	1.7-2.8	²⁸
PTPPCo/MWCNT/PP	20	1.5	0.2	1330	1.7-2.8	This work

Reference

- 1 X. He, Q. He, Y. Deng, M. Peng, H. Chen, Y. Zhang, S. Yao, M. Zhang, D. Xiao, D. Ma, B. Ge and H. Ji, *Nat. Commun.*, 2019, **10**, 3663.
- 2 B. Yu, D. J. Chen, Z. G. Wang, F. Qi, X. J. Zhang, X. Q. Wang, Y. Hu, B. Wang, W. L. Zhang, Y. F. Chen, J. R. He and W. D. He, *Chem Eng J*, 2020, **399**, 125837.
- 3 E. Cha, M. D. Patel, J. Park, J. Hwang, V. Prasad, K. Cho and W. Choi, *Nat. Nanotechnol.*, 2018, **13**, 337-344.
- 4 L. Wang, J. Liu, S. Haller, Y. Wang and Y. Xia, *Chem. Commun.*, 2015, **51**, 6996-6999.
- 5 Z. Cheng, H. Pan, J. Chen, X. Meng and R. Wang, *Adv. Energy Mater.*, 2019, **9**, 1901609.
- 6 H. Liao, H. Zhang, H. Hong, Z. Li and Y. Lin, *Electrochim. Acta*, 2017, **257**, 210-216.
- 7 L. Zhu, L. You, P. Zhu, X. Shen, L. Yang and K. Xiao, *ACS Sustainable Chem. Eng.*, 2018, **6**, 248-257.
- 8 X. Wang, W. Lei, R. Hu, P. Xia, Y. Pan, Z. Ma, N. Zhao and Y. Wang, *Ionics*, 2020, **26**, 4473-4477.
- 9 R. Ponraj, A. G. Kannan, J. H. Ahn, J. H. Lee, J. Kang, B. Han and D.-W. Kim, *ACS Appl. Mater. Interfaces*, 2017, **9**, 38445-38454.
- 10 Y. Yang, S. Wang, L. Zhang, Y. Deng, H. Xu, X. Qin and G. Chen, *Chem Eng J*, 2019, **369**, 77-86.
- 11 N. Li, W. Cao, Y. Liu, H. Ye and K. Han, *Colloids Surf., A*, 2019, **573**, 128-136.
- 12 P. Cheng, P. Guo, D. Liu, Y. Wang, K. Sun, Y. Zhao and D. He, *J Alloy Compd*, 2019, **784**, 149-156.

- 13 D. Tian, X. Song, M. Wang, X. Wu, Y. Qiu, B. Guan, X. Xu, L. Fan, N. Zhang and K. Sun, *Adv Energy Mater.*, 2019, **9**, 1901940.
- 14 Y. Zang, F. Pei, J. Huang, Z. Fu, G. Xu and X. Fang, *Adv Energy Mater.*, 2018, **8**, 1802052.
- 15 Y. Fan, Z. Niu, F. Zhang, R. Zhang, Y. Zhao and G. Lu, *ACS Omega*, 2019, **4**, 10328-10335.
- 16 Y. Song, S. Zhao, Y. Chen, J. Cai, J. Li, Q. Yang, J. Sun and Z. Liu, *ACS Appl. Mater. Interfaces*, 2019, **11**, 5687-5694.
- 17 J. Wang, P. Zhai, T. Zhao, M. Li, Z. Yang, H. Zhang and J. Huang, *Electrochim. Acta*, 2019, **320**, 134558.
- 18 X.-J. Hong, C.-L. Song, Y. Yang, H.-C. Tan, G.-H. Li, Y.-P. Cai and H. Wang, *ACS Nano*, 2019, **13**, 1923-1931.
- 19 K. Zhang, Z. Chen, R. Ning, S. Xi, W. Tang, Y. Du, C. Liu, Z. Ren, X. Chi, M. Bai, C. Shen, X. Li, X. Wang, X. Zhao, K. Leng, S. J. Pennycook, H. Li, H. Xu, K. P. Loh and K. Xie, *ACS Appl. Mater. Interfaces*, 2019, **11**, 25147-25154.
- 20 J. He, Y. Chen and A. Manthiram, *Energ Environ Sci*, 2018, **11**, 2560-2568.
- 21 G. Chen, X. Song, S. Wang, Y. Wang, T. Gao, L.-X. Ding and H. Wang, *J. Membr. Sci.*, 2018, **548**, 247-253.
- 22 Y. Lin, R. Pitcheri, J. Zhu, C. Jiao, Y. Guo, J. Li and Y. Qiu, *J Alloy Compd*, 2019, **785**, 627-633.
- 23 P. Shanthi, P. Hanumantha, T. Albuquerque, B. Gattu and P. Kumta, *ACS Appl. Energy Mater.*, 2018, **1**, 483–494.
- 24 T. Lei, W. Chen, Y. Hu, W. Lv, X. Lv, Y. Yan, J. Huang, Y. Jiao, J. Chu, C. Yan, C. Wu, Q. Li, W. He and J. Xiong, *Adv Energy Mater.*, 2018, **8**, 1802441.
- 25 J. Zhu, C. Chen, Y. Lu, J. Zang, M. Jiang, D. Kim and X. Zhang, *Carbon*, 2016, **101**, 272-280.
- 26 S. Chen, X. Han, J. Luo, J. Liao, J. Wang, Q. Deng, Z. Zeng and S. Deng, *Chem Eng J*, 2020, **385**, 123457.
- 27 Z. Li, C. Zhou, J. Hua, X. Hong, C. Sun, H.-W. Li, X. Xu and L. Mai, *Adv. Mater.*, 2020, **32**, 1907444.
- 28 N. Deng, Y. Liu, Q. Li, J. Yan, L. Zhang, L. Wang, Y. Zhang, B. Cheng, W. Lei and W. Kang, *Chem. Eng. J.*, 2019, **382**, 122918.